Available online at www.sciencedirect.com
ScienceDirect
Proceedings of the Combustion Institute 33 (2011) 905–912
Proceedings of the Combustion Institute
www.elsevier.com/locate/proci

Assessment of kinetic modeling for lean $H_2/CH_4/O_2$/diluent flames at high pressures

Michael P. Burke *, Frederick L. Dryer, Yiguang Ju

Department of Mechanical and Aerospace Engineering, Princeton University, D115 Engineering Quadrangle, Princeton, NJ 08544, USA

Abstract

Experimental measurements of burning rates, analysis of key reactions and kinetic pathways, and modeling studies were performed for $H_2/CH_4/O_2$/diluent flames spanning a wide range of fuel-lean conditions: equivalence ratios from 0.30 to 1.0, flame temperatures from 1400 to 1800 K, pressures from 1 to 25 atm, CH_4 fuel fractions from 0 to 0.1. The experimental data show negative pressure dependence of burning rate at high-pressure, low-flame-temperature conditions for all equivalence ratios and with CH_4 addition. Substantial differences are observed between literature model predictions and the experimental data as well as among model predictions themselves – up to a factor of four at high pressures. Similar to our previous work that demonstrated that none of the recent kinetic models reproduced the measured pressure dependence of the mass burning rate for all diluent concentrations and medium to high equivalence ratios, here it is demonstrated that none reproduce the measured pressure dependence for very low equivalence ratios. The effect of pressure on the kinetics of lean flames is largely driven by competition of both $H + O_2(+M) = HO_2(+M)$ and $HO_2 + O/OH/HO_2$ with the main branching reactions, in contrast to rich mixtures that are largely driven by competition of both $H + O_2(+M) = HO_2(+M)$ and $HO_2 + H$ with the main branching reactions. Methane addition is shown to influence the pressure dependence mainly through reactions of CH_3 with H and HO_2. Given the nature of the modeling problem for high-pressure flames, it appears that a rigorous solution to improving predictive capabilities will require *both* empirical adjustments of multiple rate constant parameters as well as improved characterization of the functional temperature and pressure dependence of certain highly sensitive reactions. Furthermore, many of the reactions responsible for uncertainties in the pressure dependence of H_2/O_2 flames at high pressures are shown to contribute significantly to uncertainties in the pressure dependence of flames of hydrocarbon fuels.

Keywords: Hydrogen; Methane; Syngas; Flame speed; Chemical mechanism

1. Introduction

The H_2/O_2 reaction system is a fundamental topic in combustion science that has historically received significant attention due to both its rich kinetic behavior and its importance to a variety of applications in energy conversion. Since H_2 and its intermediate oxidation species are also intermediate species in the oxidation of all hydrocarbon and oxygenated fuels, the H_2/O_2 mechanism forms an essential subset of any hydrocarbon or oxygenate oxidation mechanism [1]. And in particular,

* Corresponding author. Fax: +1 609 258 6233.
E-mail address: mpburke@princeton.edu (M.P. Burke).

1540-7489/$ - see front matter © 2010 The Combustion Institute. Published by Elsevier Inc. All rights reserved.
doi:10.1016/j.proci.2010.05.021

there has also been considerable recent interest in hydrogen-rich fuels containing CO, CO_2, H_2O, CH_4 and other small hydrocarbons (synthetic gas or "syngas") from coal or biomass gasification [2]. Typical syngas mixtures can contain significant amounts of small molecular weight hydrocarbons, particularly methane (up to 8% [2]). Combustion of syngas in gas turbine engines comprises an essential stage of Integrated Gasification Combined Cycle (IGCC) processes, which offer promise for efficient, low-emission electric power generation with increased potential for carbon capture and storage (CCS) compared to conventional coal technologies. Moreover, the combined use of biomass and coal gasification with CCS can potentially be utilized to produce both liquid transportation fuels and electrical power with net cycle carbon emissions that meet long-term goals in reducing greenhouse gas and nano-particulates [3]. In these advanced applications, operating conditions are constrained by NO_x regulations, which are frequently addressed by controlling peak temperatures through lean premixed operation and dilution to reduce in-engine NO_x formation. In addition, higher operating pressures are utilized to improve cycle efficiency. This paper addresses the burning rate behavior of high-hydrogen-content fuels containing methane under these operating conditions.

Measurements of pure H_2, H_2/CO, and H_2/CH_4 burning velocities have been mostly studied at low pressures (below 5 atm). Measurements of pure H_2 ([4–6]) and H_2/CO ([6–9]) burning velocities at high pressures are relatively sparse. In recent work, we have shown discrepancies of a factor of three in burning rate predictions for near-stoichiometric and rich H_2/O_2/diluent and H_2/CO/O_2/diluent flames at high pressures and low flame temperatures using recently published kinetic models. Furthermore, we found that none of the various kinetic models in the literature predict the pressure dependence observed for all diluent concentrations and all equivalence ratios from 0.85 to 2.5.

We consider experimental data for leaner mixtures to be useful for two main reasons: (1) to provide validation targets at conditions closer to applications and (2) to de-convolve the sources of model disagreement to ensure that future modeling solutions are not limited to higher equivalence ratios, where a different set of reactions is important. For example, the reactions of HO_2 with H that dominate HO_2 consumption and the pressure dependence at rich conditions are replaced by the reactions of HO_2 with OH, HO_2, and O at lean conditions. Furthermore, we show that the presence of methane in high hydrogen syngas has substantial effects on the coupling of these important reaction paths.

The objectives of the present study are threefold. First, we test the performance of recent kinetic models for H_2 [10–16] and C_1 or above [12,16,17] for flame conditions relevant to syngas applications. We present flow-corrected burning rates from outwardly propagating flames for H_2/CH_4/O_2/He mixtures over wide ranges of sub-unity equivalence ratios, pressures, flame temperatures, and with and without CH_4 addition at perturbation levels of interest to syngas applications. We focus our study on low-flame-temperature conditions (from 1400 to 1800 K) of practical interest to advanced engine applications to achieve low NO_x emissions. Second, we identify the changing kinetic pathways in H_2/CH_4/O_2/He flames as pressure is increased to gain a better understanding of the fundamental kinetic phenomena in high-pressure flames. Third and finally, we discuss approaches to resolving the modeling problem posed by dilute, high-pressure H_2 flames and demonstrate that its resolution is also essential to predicting of high-pressure flames of hydrocarbons.

2. Experimental and numerical methods

Details of the experimental apparatus can be found in Refs. [18,19]. The experimental procedure, data analysis, and estimation of uncertainties are nearly identical to that used in [6]. High-speed Schlieren photography was utilized to record the propagation of outwardly propagating flames in a dual-chambered, pressure-release type high-pressure combustion apparatus. The instantaneous flame speed and stretch rate were calculated using a flow-correction method [19]. Extrapolation to the unstretched burning velocity was achieved using the linear stretch relation [20]. A complete list of initial conditions (mixture composition, temperature, and pressure), exact ranges used for analysis, derived burning velocity and mass burning rate values, and estimated uncertainties for each measurement are reported in Table S1 in the Supplementary data. Mass burning rate predictions from the various models tested [10–17] were calculated from planar, adiabatic flame simulations with multi-component transport and Soret diffusion [21].

3. Results

3.1. Effect of pressure and flame temperature

Experiments were conducted over a wide range of sub-unity equivalence ratios, dilution ratios, and pressures. Mass burning rates, defined as $f^o = \rho_u s_u^o$, where ρ_u is the unburned gas density and s_u^o the burning velocity, are presented here since they are typically more illuminating of the global chemistry. As indicated by Egolfopoulos and Law [22], the pressure dependence of the mass burning rate is more directly related to the pres-

sure dependence of the global reaction rate than is the flame speed.

Mass burning rates measured for $H_2/O_2/He$ mixtures of equivalence ratio of 0.70 for a variety of pressures and dilution levels are presented in Fig. 1 (and Fig. S1 in the Supplementary data). Dilution levels were adjusted to achieve flame temperatures near 1400, 1600, and 1800 K. Above about 10 atm, flames are observed to be strongly affected by buoyancy for flame temperatures near 1400 K, and instabilities develop quickly after ignition for flame temperatures near 1800 K. The pressure dependence of the burning rate is experimentally observed to be positive at lower pressures. However, at nominal flame temperatures of 1400 and 1600 K, the pressure dependence becomes negative at higher pressure. The maximum burning rate moves to lower pressures as flame temperature decreases. Similar negative pressure dependence of burning rates has been experimentally observed previously in N_2-diluted CH_4–air flames [22] and near-stoichiometric and rich $H_2/CO/O_2$/diluent flames [6].

At atmospheric pressure, burning rate predictions using recently published chemical kinetic models agree reasonably well with one another and the experimental data. However, at higher pressures, the predicted mass burning rates using published models differ substantially from the experimental data and from one another. Much larger disparities are apparent among the model predictions at lower flame temperatures, with variations of a factor of 2.5 for a flame temperature near 1800 K and up to a factor of 4.0 near 1400 K. The model of Konnov over-predicts the burning rate by a factor of two and GRI-MECH 3.0 under-predicts the burning rate by a factor of two, while the models of Davis et al. and O'Connaire et al. predict the observed burning rate within 20% across the conditions spanned in Fig. 1 and Fig. S1. Predictions of the models [10,11,13,14,16] were also compared to the experimental data of Bradley et al. [5] for lean H_2/air mixtures up to 10 atm. The comparison reveals similarly large disagreement between experimental data and model predictions, as well as among model predictions, at high pressures and low equivalence ratios (which also correspond to low flame temperatures).

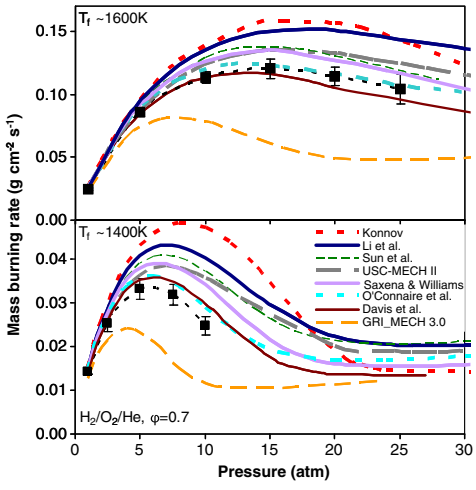

Fig. 1. Pressure dependence of mass burning rates for $H_2/O_2/He$ flames of equivalence ratio 0.70 for various He concentrations. Symbols show experimental data. Lines show predictions from models considered in this study [10–16]. For ease in viewing predictions, the models are ranked (approximately) in the legend from highest to lowest burning rate.

3.2. Effect of equivalence ratio

Experiments were conducted across a range of sub-unity equivalence ratios with dilution varied for each equivalence ratio such the adiabatic flame temperature is approximately constant (in order to separate the two effects). The measurements are compared with the predictions from the models of Davis et al. [11], O'Connaire et al. [14], and Li et al. [10] (not shown in figures for clarity). For flame temperatures near 1600 K (shown in Fig. S2 in the Supplementary data), the models of Davis et al. and O'Connaire et al. predict the observed burning rates for equivalence ratio variation within ~15%, and the model of Li et al. predicts within ~30%. For flame temperatures near 1400 K (shown in Fig. 2), the models accurately predict the observed trends at 1 atm. However, they predict opposite qualitative trends at 5 atm and overpredict the experimental data at 10 atm. Disagreement of the models of Davis et al., O'Connaire et al., and Li et al. with the experimental data at an equivalence ratio 0.30 approach ~30%, 30%, and 75%, respectively. Figure 3 reveals that none of the kinetic models accurately predict the observed burning rate pressure dependence for this very lean mixture.

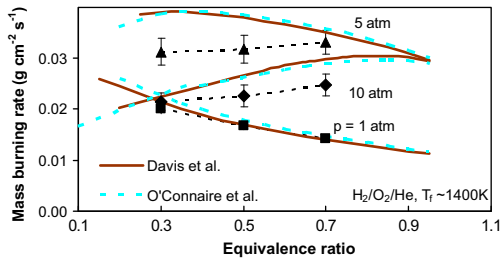

Fig. 2. Mass burning rates for $H_2/O_2/He$ flames of various equivalence ratios with dilution adjusted to achieve flame temperatures near 1400 K for different pressures. Symbols show experimental data. Lines show predictions from models [11,14].

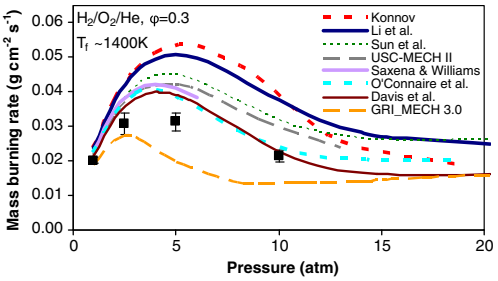

Fig. 3. Pressure dependence of mass burning rates for H_2/O_2/He flames of equivalence ratio 0.30 and flame temperature near 1400 K. Symbols show experimental data. Lines show predictions from models considered in this study [10–16]. For ease in viewing predictions, the models are ranked (approximately) in the legend from highest to lowest burning rate.

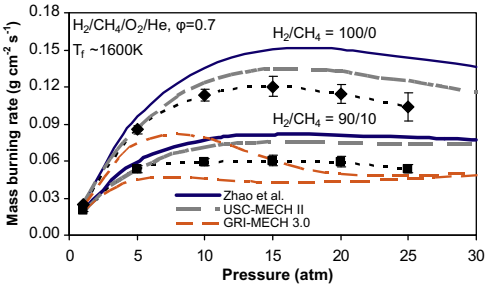

Fig. 4. Pressure dependence of mass burning rates for $H_2/CH_4/O_2$/He flames of equivalence ratio 0.70 for $H_2/CH_4 = 100/0$ and 90/10 with He concentration adjusted to achieve flame temperatures near 1600 K. Symbols show experimental data. Lines show predictions from models considered in this study [12,16,17]. For ease in viewing predictions, the models are ranked (approximately) in the legend from highest to lowest burning rate.

3.3. Effect of CH_4 addition to the fuel

Mass burning rates were measured for $H_2/CH_4/O_2$/He mixtures at an equivalence ratio of 0.70 and a variety of pressures (Fig. 4). Dilution was adjusted for both H_2/CH_4 ratios to achieve flame temperatures near 1600 K. The burning rate pressure dependence of the $H_2/CH_4 = 90/10$ and $H_2/CH_4 = 100/0$ mixtures are nearly the same, displaying a positive gradient at low pressures and a negative gradient at high pressures. The reduction in burning rate with increasing CH_4 addition is observed to be stronger at higher pressures. While the reduction increases from 20% at 1 atm to 60% at 5 atm, a factor of two reduction that is nearly independent of pressure is observed at higher pressures (~10–25 atm).

4. Analysis and discussion

4.1. Analysis of controlling reactions and kinetic pathways

Presented below are results from kinetic analyses performed using the models of Li et al. [10] and Zhao et al. [17] (which uses the H_2 model from Li et al.) to allow straightforward comparison with the analyses presented in our previous work [6] where the model of Li et al. is used. Similar observations were obtained using USC-MECH II [12] (which uses the H_2/CO model from Davis et al. [11] with recent updates) for the analysis.

Predicted species profiles and reaction fluxes were analyzed for H_2/O_2/He flames of equivalence ratios of 0.3, 1.0, and 2.5 with flame temperatures near 1400 K at 1, 5 and 10 atm to ascertain the effect of pressure and equivalence ratio on the flame structure and kinetic pathways. The primary cause for the pressure and temperature dependence appears to be the competition of the pressure-dependent recombination reaction $H + O_2(+M) = HO_2(+M)$ (R1) and strongly temperature-dependent chain-branching reaction $H + O_2 = OH + O$ (R2), though the exact nature of the dependence is also influenced by HO_2 consumption pathways. (See Table 1 for a list of pertinent reactions.) At conditions where HO_2 is relatively unreactive, (R1) effectively removes active radicals, while (R2) participates in a chain-branching cycle with $O + H_2 = OH + H$ (R3) and $OH + H_2 = H_2O + H$ (R4) to essentially produce three H atoms for every H atom destroyed. If (R1)–(R4) are considered and (R1) is assumed to be terminating, the overall branching ratio is responsible for the well-known second limit in homogeneous kinetics, $2k_2/k_1[M] = 1$ [23]. At pressures above the third explosion limit and lower temperatures such that $2k_2/k_1[M] < 1$, H_2O_2 formation from HO_2 and its subsequent decomposition and/or reaction allows for a chain-carrying reaction sequence that is thermally self-accelerative in contrast to (faster) chain-explosive kinetics [24]. Consequently, even for

Table 1
List of reactions discussed in the text.

(R1)	$H + O_2(+M) = HO_2(+M)$
(R2)	$H + O_2 = OH + O$
(R3)	$O + H_2 = OH + H$
(R4)	$OH + H_2 = H_2O + H$
(R5)	$H + HO_2 = H_2 + O_2$
(R6)	$H + HO_2 = OH + OH$
(R7)	$HO_2 + OH = H_2O + O_2$
(R8)	$HO_2 + O = O_2 + OH$
(R9)	$HO_2 + HO_2 = H_2O_2 + O_2$
(R10)	$O + H_2O = OH + OH$
(R11)	$CO + OH = CO_2 + H$
(R12)	$CH_3 + HO_2 = CH_3O + OH$
(R13)	$CH_3 + H(+M) = CH_4(+M)$
(R14)	$O + OH + M = HO_2 + M$

pressures above the third limit, the second limit plays an important role in terms of characteristic reaction times and is generally referred to as the "extended second limit" [24,25]. However, as shown by Baldwin and co-workers (e.g., [26]), consideration of gas-phase consumption of HO_2 is necessary to predict explosion limit behavior when heterogeneous radical destruction is suppressed. For the flame conditions studied here, HO_2 is consumed almost exclusively by reactions (e.g., see Fig. 6) with radical species that are radical chain-carrying or terminating. Therefore, for these flames as well as most kinetic systems, increased flux through HO_2 kinetic pathways inhibits the overall reaction rate.

The demarcation of kinetic regimes imposed by the extended second limit has been observed for H_2 oxidation in flow reactor species profiles [24] and counterflow ignition studies [25]. The competition between (R1) and (R2) along with the subsequent competition among the chain-branching and terminating reactions that affect the extended second limit are principally responsible for the burning rate pressure dependence of flames.

The effect of pressure on the flame structure based on the flux of H atoms through (R1) and (R2), as well as H atom mole fraction, is illustrated in Fig. 5 for an equivalence ratio of 0.3. While numerous reactions contribute to defining the extended second limit, especially for lean conditions, the temperature where $2k_2/k_1[M] = 1$ is plotted in this figure as indicator for the extended second limit for the given pressures. The results indicate that with increasing pressure, the temperature of extended second limit increases accordingly for both lean and rich mixture conditions. Therefore, the portion of the flame that undergoes strong branching kinetics (i.e., at temperatures above the extended second limit) is reduced to a narrower temperature-window approaching the adiabatic flame temperature at higher pressures. All radical and reaction flux profiles shift to a narrower higher temperature region at high pressures – indicating a higher overall activation energy. As pressure is increased, the flux through (R1) relative to (R2) is increased, producing more HO_2 instead of O and OH. The higher HO_2 concentrations lead to increased competition between HO_2 pathways and strong branching channels at high pressures.

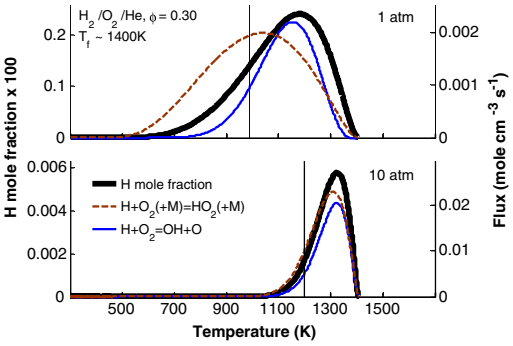

Fig. 5. H radical mole fraction and H consumption by (R1) and (R2) for H_2/O_2/He flames of equivalence ratio 0.30 with flame temperature near 1400 K. Vertical lines mark the temperature where $2k_2/k_1 = 1$ for the given pressures.

The specific reactions that consume HO_2 and those that influence the pressure dependence strongly vary with equivalence ratio. The consumption pathways for HO_2 at 10 atm for equivalence ratios of 0.3, 1.0, and 2.5 are displayed in Fig. 6. For equivalence ratio 2.5 where there is excess H_2, reactions with H_2, namely, (R3) and (R4), dominate the consumption of O and OH, respectively. The radical pool is primarily comprised of H and HO_2. Consequently, reactions with H, namely $H + HO_2 = H_2 + O_2$ (R5) and $H + HO_2 = OH + OH$ (R6), are responsible for nearly all HO_2 consumption. The pressure dependence is governed by competition between two pairs of competing reaction channels, (R1) vs. (R2) and (R5) vs. (R6), which are responsible for nearly all H consumption. A-factor sensitivity analysis conducted at 1, 5 and 10 atm for equivalence ratio 2.5 reveals that the rate constants of these four reactions are the most sensitive and that their sensitivities increase substantially with pressure.

For equivalence ratio 0.30 where there is excess O_2, reactions with O_2, namely (R1) and (R2), contribute to nearly all of the H consumption. Concentrations of all radical species are the same order of magnitude, but H is the least abundant. As shown in Fig. 6, HO_2 is primarily consumed by reaction (R7) with OH (48%), reaction (R8) with O (23%), and reaction (R9) with HO_2 (10%), such that reactions (R5) and (R6) with H account for only 15% and 3% of HO_2 consumption. For O consumption, (R3) competes with (R8) and $O + H_2O = OH + OH$ (R10) as the peak radical concentrations are shifted towards the

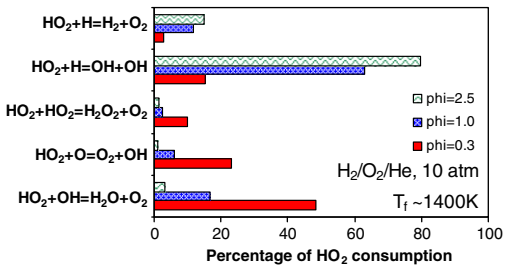

Fig. 6. Consumption pathways of HO_2 in H_2/O_2/He flames at 10 atm for various equivalence ratios with dilution varied to achieve flame temperatures near 1400 K.

post-flame region where more H_2O is present; for OH consumption, (R4) competes with (R7). A-factor sensitivity analysis of the burning rate conducted at 1, 5 and 10 atm for equivalence ratio 0.3 is shown in Fig. 7. The results indicate that that the pressure dependence is governed by (R1) and (R2) which compete for H, (R3), (R8) and (R10) which compete for O, (R4) and (R7) which compete for OH, and (R9) which competes with (R7) and (R8) for HO_2. While (R6) exhibits relatively high sensitivity, the importance of the $H + HO_2$ channels is substantially reduced compared to rich conditions.

For equivalence ratio 1.0 where there is neither excess H_2 nor excess O_2, HO_2 is substantially consumed by many of the reactions shown in Fig. 6. Consequently, competition among all competing reactions is important as indicated by the high sensitivity indices that increase with pressure for all the reactions important for lean and rich conditions.

A-factor sensitivity analysis for the burning rate of the $H_2/CH_4 = 90/10$ mixture of equivalence ratio 0.70 in Fig. 4 at different pressures reveals nearly identical reaction sensitivity ranking, pressure dependences, and magnitudes as for a pure H_2 mixture. The three most notable exceptions are that $CO + OH = CO_2 + H$ (R11), $CH_3 + HO_2 = CH_3O + OH$ (R12), and $CH_3 + H (+M) = CH_4(+M)$ (R13) are relatively sensitive for these perturbation levels of CH_4. In terms of the effect on the radical pool, (R11) and (R4) are equivalent paths – each consume a fuel-molecule/fragment and OH and produce a stable product and H. Whereas, (R12) is chain-carrying reaction that consumes HO_2 and (R13) is a chain-terminating reaction that consumes H. While (R12) and (R13) compete more strongly with (R5)–(R9) and (R1)–(R2), respectively, and are more sensitive with increased CH_4 addition, reactions (R1), (R2), and many of the other HO_2 consumption reactions (R5)–(R9) are important even for much higher CH_4 fuel fractions – suggesting that (R1), (R2) and (R5)–(R9) might also play a prominent role in the pressure dependence of hydrocarbon flames as well, as is demonstrated below.

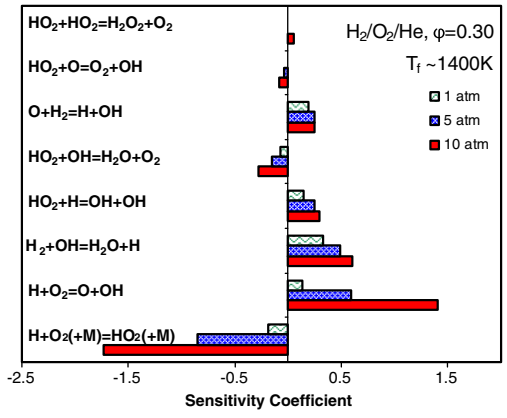

Fig. 7. Sensitivity of mass burning rate to A-factors of elementary rate constants for H_2/O_2/He flames of equivalence ratio 0.3 with flame temperature near 1400 K for various pressures.

4.2. Description of modeling problem and suggested approach to a rigorous solution

The observed discrepancies between model predictions [10–17] and experiments and among model predictions themselves are noteworthy. All of the H_2 models tested here [10–11,13–15] have been validated against extensive (and frequently the same) sets of data including high-pressure burning rates [4]. Furthermore, many of the most sensitive reactions for the present conditions are highly sensitive reactions in a wide variety of combustion systems, both for H_2 and other hydrocarbons. At present, the uncertainties at these conditions can be attributed to a number of sources, including the temperature dependence of rate constants for $HO_2 + O/OH/HO_2/H$ reactions, fall-off behavior for (R1) in both pure and mixed bath gases, and rate constants for reactions, like $O + OH + M = HO_2 + M$ (R14), which have typically been ignored but can affect predictions using rate constants within uncertainty limits. Similar to our previous work [6], analyses suggest that H atom diffusion contributes to the present uncertainties somewhat but is not the sole source of disagreement. We refer the reader to Ref. [6] for more detailed description of the present uncertainties, which we do not elaborate upon here.

It appears that a solution to the present modeling problem will likely require two concurrent efforts: (1) empirical fitting of model parameters to match validation targets (like burning rates) that depend on the entire *system of reactions* and (2) improved understanding of the temperature and pressure dependence of certain highly sensitive *single elementary reactions*. Figures 7 and 8 illustrate the two facets of the present modeling challenge. For the lean H_2/O_2/He mixture at 10 atm in Fig. 7, the sensitivity coefficient is 1.5 for (R2), one of the best characterized reactions in combustion. Assuming (R2) was known within 10% (best precision in elementary rate measurements under "favorable circumstances"), 25% (present estimated uncertainty at 800 K), 60% (present estimated uncertainty at 3500 K) [27], and linear sensitivity to (R2), the uncertainty in this rate constant alone leads to an uncertainty in the burning rate of 15%, 40%, and 80%, respectively. In fact, applying 10% uncertainties in every rate constant (and assuming linear sensitivities) yields burning rate uncertainties of ~30% – far beyond what is typically considered good agreement for burning rates. Therefore, even under

favorable circumstances, improvements to rate parameter accuracies from elementary reaction studies will not yield the level of accuracy typically expected for predictions that involve the entire system of reactions, such as in the present flames. Achieving better predictive accuracy at these conditions must rely on adjustments of model parameters to reproduce high pressure burning rates, such as those adjustments of Refs. [10,11,14]. Further, consideration of a large set of burning rate data that spans a wide range of pressures, upstream temperatures, flame temperatures, and equivalence ratios will be necessary to ensure modeling solutions that are not as limited in range of applicability as previously.

At the same time, the parameters that describe the temperature and pressure dependence for some reactions, or even the functional form of the temperature and pressure dependence for some reactions, are not well known. For example, (R7) is thought to have a highly non-Arrhenius temperature dependence that exhibits an order of magnitude reduction in the rate constant at temperatures around 800–1200 K [28,29]. Figure 8 illustrates the effect of using different rate constant expressions for (R7) [30] that have different temperatures for the rate constant minimum and different profiles – yielding as much as a 60% difference in predicted flame speed (that is highly condition dependent). Present parameter adjustment/optimization techniques for model development, such as [10,11,14], are incapable of handling uncertainties in the temperature and pressure dependence of elementary reactions. (Furthermore, the strongly coupled interactions of many model parameters at these conditions would make discerning the functional dependence of a rate constant like that of (R7) from high-pressure burning rate data very difficult if not impossible.)

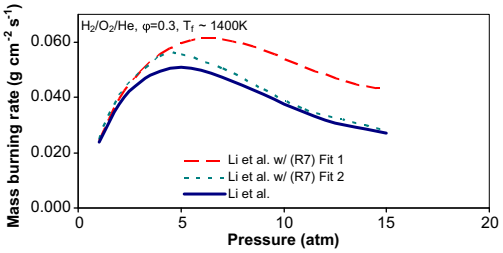

Fig. 8. Comparison of experimental data with predictions using the model of Li et al. and modified versions of Li et al. where different rate expressions for (R7) are substituted. Fit 1 is the rate constant expression from Chaos and Dryer [30] to the experimental data of Hippler et al. [28], which exhibit a rate constant minimum near 1200 K. Fit 2 is the rate constant expression from Chaos and Dryer [30] to the experimental data of Kappel et al. [29], which exhibit a rate constant minimum near 1000 K.

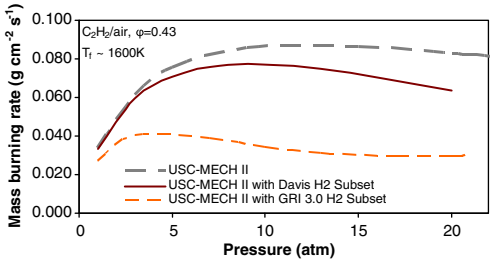

Fig. 9. Mass burning rate predictions for a C_2H_2/air mixture of equivalence ratio 0.43 using USC-MECH II [12], a modified version of USC-MECH II where the H_2 subset from Davis et al. [11] is substituted, and a modified version of USC-MECH II where the H_2 subset from GRI 3.0 [16] is substituted. The main difference between the H_2 subsets of USC-MECH II and Davis et al. is the rate constant for (R7), and USC-MECH II and GRI 3.0 (R1).

Therefore, improved characterization of highly sensitive elementary reactions through more isolated studies is also essential to improving predictive capability.

4.3. Implications for kinetic modeling of hydrocarbon flames at high pressures

Analyses of flame simulations were conducted for a variety of fuels, including butane, acetylene, and toluene, in air with sub-unity equivalence ratios varied to achieve flame temperatures near 1600 K. The analysis reveals increased sensitivity to elementary rate constants for (R1), (R2), and (R7) at high pressures. To illustrate the effect that the present uncertainties in the H_2/O_2 kinetics have on flame predictions for hydrocarbon fuels, predicted burning rates are plotted in Fig. 9 for acetylene–air flames of equivalence ratio 0.43 using three versions of USC-MECH II [12] – one using the original H_2 subset, one using the H_2 subset from Davis et al. [11], and one using the H_2 subset from GRI-MECH 3.0 [16]. The results demonstrate a substantial impact of the H_2 subset used for these predictions and the importance of (R1), (R2), and (R7) in high-pressure flames for fuels beyond hydrogen.

5. Conclusions

Experimental measurements of burning rates, analysis of the key reactions and kinetic pathways, and modeling studies were performed for H_2/CH_4/O_2/diluent flames spanning a wide range of fuel-lean conditions. The experimental data show negative pressure dependence of burning rate at high-pressure, low-flame-temperature conditions for all equivalence ratios and with CH_4 addition. Substantial differences are observed between liter-

ature model predictions and the experimental data as well as among model predictions themselves – up to a factor of four at high pressures. None of the recent kinetic models reproduce the measured pressure dependence for very lean mixtures. The effect of pressure on the kinetics of lean flames is largely driven by competition of $H + O_2(+M) = HO_2(+M)$ and HO_2 reactions with radical species, which are strongly dependent on equivalence ratio, with the main branching reactions. It appears that a rigorous solution to the modeling problem will likely both empirical adjustments of multiple rate constant parameters as well as improved characterization of the functional temperature and pressure dependence of certain highly sensitive reactions. Furthermore, many of the reactions responsible for the uncertainties in the pressure dependence of H_2/O_2 flames at high pressures are shown to contribute significantly to uncertainties in the pressure dependence of flames of hydrocarbon fuels.

Acknowledgements

This work was supported by the following awards: Award Number DE-NT0000752 funded by the US Department of Energy through the University Turbine Systems Research (UTSR) Program (F.L.D., Y.J); "From Fundamentals to Multi-scale Predictive Models for 21st Century Transportation Fuels," an Energy Frontier Research Center funded by the US Department of Energy, Office of Science, Office of Basic Energy Sciences under Award Number DE-SC0001198 (F.L.D., Y.J); and Siemens Power Generation, Inc., (technical monitor: Dr. Scott Martin) (F.L.D.).

Appendix A. Supplementary data

Supplementary data associated with this article can be found, in the online version, at doi:10.1016/j.proci.2010.05.021.

References

[1] C.K. Westbrook, F.L. Dryer, *Prog. Energ. Combust. Sci.* 10 (1984) 1–57.
[2] G.A. Richards, K.H. Casleton, N.T. Weiland, *Syngas Utilization*, in: T.C. Lieuwen, V. Yang, R.A. Yetter (Eds.), *Synthesis Gas Combustion: Fundamentals and Applications*, Taylor and Francis, 2009, pp. 193–222.
[3] E.D. Larson, G. Fiorese, G. Liu, R.H. Williams, T.G. Kreutz, S. Consonni, *Energy Environ. Sci.* 3 (2010) 28–42.
[4] S.D. Tse, D.L. Zhu, C.K. Law, *Proc. Combust. Inst.* 28 (2000) 1793–1800.
[5] D. Bradley, M. Lawes, K. Liu, S. Verhelst, R. Woolley, *Combust. Flame* 149 (2007) 162–172.
[6] M.P. Burke, M. Chaos, F.L. Dryer, Y. Ju, *Combust. Flame* 157 (2010) 618–631.
[7] H.Y. Sun, S.I. Yang, G. Jomaas, C.K. Law, *Proc. Combust. Inst.* 31 (2007) 439–446.
[8] J. Natarajan, T. Lieuwen, J. Seitzman, *Combust. Flame* 151 (2007) 104–119.
[9] J. Natarajan, Y. Kochar, T. Lieuwen, J. Seitzman, *Proc. Combust. Inst.* 32 (2009) 1261–1268.
[10] J. Li, Z. Zhao, A. Kazakov, F.L. Dryer, *Int. J. Chem. Kinet.* 36 (2004) 566–575.
[11] S.G. Davis, A. Joshi, H. Wang, F.N. Egolfopoulos, *Proc. Combust. Inst.* 30 (2005) 1283–1292.
[12] H. Wang, X. You, A.V. Joshi, et al., USC Mech Version II. High-temperature Combustion Reaction Model of H2/CO/C1-C4 Compounds. <http://ignis.usc.edu/USC_Mech_II.htm/>, May 2007.
[13] A.A. Konnov, *Combust. Flame* 152 (2008) 507–528.
[14] M. O'Connaire, H.J. Curran, J.M. Simmie, W.J. Pitz, C.K. Westbrook, *Int. J. Chem. Kinet.* 36 (2004) 603–622.
[15] P. Saxena, F.A. Williams, *Combust. Flame* 145 (2006) 316–323.
[16] G.P. Smith, D.M. Golden, M. Frenklach, et al., GRI-MECH 3.0. Available at: <http://www.me.berkeley.edu/gri_mech/>.
[17] Z. Zhao, M. Chaos, A. Kazakov, F.L. Dryer, *Int. J. Chem. Kinet.* 40 (2008) 1–18.
[18] X. Qin, Y. Ju, *Proc. Combust. Inst.* 30 (2005) 233–240.
[19] M.P. Burke, Z. Chen, Y. Ju, F.L. Dryer, *Combust. Flame* 156 (2009) 771–779.
[20] G.H. Markstein, *Non-Steady Flame Propagation*, Pergamon, New York, 1964, p. 22.
[21] J.R. Kee, F.M. Rupley, J.A. Miller, *Sandia National Laboratories Report SAND 89–8009B*, Livermore, CA, 1992.
[22] F.N. Egolfopoulos, C.K. Law, *Combust. Flame* 80 (1990) 7–16.
[23] B. Lewis, G. von Elbe, *Combustion, Flames and Explosions of Gases*, third ed., Academic Press, Orlando, 1987.
[24] M.A. Mueller, T.J. Kim, R.A. Yetter, F.L. Dryer, *Int. J. Chem. Kinet.* 31 (1999) 113–125.
[25] X.L. Zheng, C.K. Law, *Combust. Flame* 136 (2004) 168–179.
[26] R.R. Baldwin, R.W. Walker, *J. Chem. Soc., Faraday Trans.* 75 (1979) 140–154.
[27] D.L. Baulch, C.T. Bowman, C.J. Cobos, et al., *J. Phys. Chem. Ref. Data* 34 (3) (2005) 757–1397.
[28] H. Hippler, H. Neunaber, J. Troe, *J. Phys. Chem.* 103 (1995) 3510–3516.
[29] Ch. Kappel, K. Luther, J. Troe, *Phys. Chem. Chem. Phys.* 4 (2002) 4392–4398.
[30] M. Chaos, F.L. Dryer, *Combust. Sci. Technol.* 180 (2008) 1051–1094.